Molecular Mechanism of Lipid Nanodisk Formation by Styrene-Maleic Acid Copolymers

Xue, Minmin; Cheng, Lisheng; Faustino, Ignacio; Guo, Wanlin; Marrink, Siewert J

Published in:
Biophysical Journal

DOI:
10.1016/j.bpj.2018.06.018

Publication date:
2018

Molecular Microbiology (2018) 109(3), 278–290 ■
doi:10.1111/mmi.14008
First published online 20 June 2018

Assessment of the interaction between the flux-signaling metabolite fructose-1, 6-bisphosphate and the bacterial transcription factors CggR and Cra

Brenda Bley Folly,[1] Alvaro D. Ortega,[1,2*] Georg Hubmann,[1] Silke Bonsing-Vedelaar,[1] Hein J. Wijma,[3] Pieter van der Meulen,[4] Andreas Milias-Argeitis[1] and Matthias Heinemann[1*]

[1]*Molecular Systems Biology, Groningen Biomolecular Sciences and Biotechnology Institute, University of Groningen, Nijenborgh 4, 9747 AG, Groningen, The Netherlands.*
[2]*Department of Cell Biology, Faculty of Biology, Complutense University of Madrid, José Antonio Nováis 12, 28040, Madrid, Spain.*
[3]*Biotechnology, Groningen Biomolecular Sciences and Biotechnology Institute, University of Groningen, Nijenborgh 4, 9747 AG, Groningen, The Netherlands.*
[4]*Stratingh Institute for Chemistry, University of Groningen, Nijenborgh 4, 9747 AG, Groningen, The Netherlands.*

Summary

Bacteria regulate cell physiology in response to extra- and intracellular cues. Recent work showed that metabolic fluxes are reported by specific metabolites, whose concentrations correlate with flux through the respective metabolic pathway. An example of a flux-signaling metabolite is fructose-1,6-bisphosphate (FBP). In turn, FBP was proposed to allosterically regulate master regulators of carbon metabolism, Cra in *Escherichia coli* and CggR in *Bacillus subtilis*. However, a number of questions on the FBP-mediated regulation of these transcription factors is still open. Here, using thermal shift assays and microscale thermophoresis we demonstrate that FBP does not bind Cra, even at millimolar physiological concentration, and with electrophoretic mobility shift assays we also did not find FBP-mediated impairment of Cra's affinity for its operator site, while fructose-1-phosphate does. Furthermore, we show for the first time that FBP binds CggR within the millimolar physiological concentration range of the metabolite, and decreases DNA-binding activity of this transcription factor. Molecular docking experiments only identified a single FBP binding site CggR. Our results provide the long thought after clarity with regards to regulation of Cra activity in *E. coli* and reveals that *E. coli* and *B. subtilis* use distinct cellular mechanism to transduce glycolytic flux signals into transcriptional regulation.

Accepted 13 June, 2018. *For correspondence. E-mail m.heinemann@rug.nl, alvort05@ucm.es.

Introduction

Microorganisms display mechanisms that sense metabolic fluxes and translate this flux information into a cellular response (Fung *et al.*, 2005; Kotte *et al.*, 2010). Specifically, the concentrations of certain so-called flux-signaling metabolites correlate with the flux through the respective metabolic pathway (Litsios *et al.*, 2017). A recognized flux-signaling metabolite is the glycolytic intermediate fructose-1,6-bisphosphate (FBP), whose concentration linearly correlates with the flux through glycolysis in *Bacillus subtilis* (Chubukov *et al.*, 2013) and *Escherichia coli* (Kotte *et al.*, 2010; Kochanowski *et al.*, 2013), dynamically varying in a broad concentration range: from 0.01 mM to around 15 mM (Bennett *et al.*, 2009; Kleijn *et al.*, 2009; Meyer *et al.*, 2014; Link *et al.*, 2015; Kochanowski *et al.*, 2017). The flux-signal imprinted in the concentration of FBP is then used to exert flux-dependent actions, for instance, flux-dependent allosteric regulation of transcription factors (TFs) or metabolic enzymes (Murcott *et al.*, 1992; Cameron *et al.*, 1994; Ormö *et al.*, 1998; Yu and Pettigrew, 2003; Dombrauckas *et al.*, 2005).

In particular, it has been reported that FBP regulates two pleiotropic TFs that have a central role in the glycolytic switch by controlling the expression of numerous genes involved in carbon metabolism in bacteria. In *E. coli*, Cra (Catabolite repressor/activator) activates the transcription of genes encoding biosynthetic and

oxidative enzymes involved in the Krebs cycle, glyoxylate shunt and gluconeogenesis, and represses the transcription of genes involved in glycolysis (Ramseier *et al.*, 1993; Bledig and Ramseier, 1996; Saier and Ramseier, 1996; Chavarría *et al.*, 2011). In *B. subtilis,* CggR inhibits the transcription of the *gapA* operon, which encodes the five enzymes catalyzing the central part of glycolysis and *cggR* gene (Ludwig *et al.*, 2001). Cells grown in glycolytic carbon sources induce *gapA* transcription in response to a signal arising from central glycolysis that alleviates CggR-mediated repression (Doan and Aymerich, 2003). According to our current knowledge, the interaction of FBP with the TFs impairs the affinity for their operator sequences (Ramseier *et al.*, 1993; Doan and Aymerich, 2003), which would lead to the de-repression of target operons. However, so far a direct proof for the interactions between FBP at its physiological concentration range and these two TFs has not been revealed.

Recently, we found that in glucose-limited chemostat cultures Cra activity decreases with glycolytic flux while FBP levels increase (Kochanowski *et al.*, 2013), which is consistent with the presumed inactivation of Cra by FBP. While the precise molecular mechanism is still obscure, Ramseier reported that 5 mM FBP partially displaced Cra-binding from the *ppsA* promoter *in vitro* (Ramseier *et al.*, 1993), a result that the same authors claimed also for handful of other Cra target genes (Ramseier *et al.*, 1995). In contrast, a recent comprehensive *in silico, in vitro* and *in vivo* analyses of the putative regulation by FBP of the homologue of Cra in *Pseudomonas putida* found only evidence for fructose-1-phosphate (F1P) binding to Cra, but not FBP (Chavarría *et al.*, 2011; Chavarría *et al.*, 2014). However, because of the significant differences between upper glycolysis in *P. putida* and *E. coli* the regulation of Cra in these organisms might be also different. More recently, mutants of Cra were reported to display affinities for FBP from nano to low micromolar range (Wei *et al.*, 2016; Zhu *et al.*, 2016). However, these authors could not find a significant effect of these mutations on either the regulation Cra's DNA-binding activity *in vitro* or on transcriptional control of its targets *in vivo* (Wei *et al.*, 2016; Zhu *et al.*, 2016), which casts doubts about the specificity and the functional consequences of the alleged change in Cra's affinity for FBP. Therefore, although it has been widely assumed that FBP regulates Cra in *E. coli* (Ramseier *et al.*, 1993; Ramseier *et al.*, 1995; Saier and Ramseier, 1996; Kotte *et al.*, 2010; Kochanowski *et al.*, 2013; Chubukov *et al.*, 2014; Lehning *et al.*, 2017), a definite experimental and functionally relevant proof of the interaction between FBP and Cra is still missing.

Also for CggR, there are a number of open questions. Using fluorescence anisotropy and isothermal calorimetry it has been consistently demonstrated that FBP binds CggR with high affinity (K_D 2–7 μM) (Zorrilla, Chaix, *et al.*, 2007; Řezáčová *et al.*, 2008). This interaction reduces the size of CggR oligomers and stabilizes dimers against denaturation but has no effect on DNA-binding activity (Zorrilla, Chaix, *et al.*, 2007). In addition, different phosphorylated sugars (and even inorganic phosphate) can also bind FBP-binding site without triggering the induction response (Řezáčová *et al.*, 2008). In fact, it is necessary to add millimolar concentrations of FBP to affect CggR affinity for its operator by impairing the cooperativity in CggR-DNA interaction (Doan and Aymerich, 2003; Zorrilla, Chaix, *et al.*, 2007), which led to hypothesize the occurrence of a second low affinity FBP-binding site that would be responsible for FBP-mediated allosteric regulation of the TF (Doan and Aymerich, 2003; Zorrilla, Doan, *et al.*, 2007; Chaix *et al.*, 2010). However, this low affinity FBP-binding site could not be unveiled in CggR co-crystallized in the presence of 90 mM FBP (Řezáčová *et al.*, 2008), and therefore, the mechanism by which FBP regulates CggR activity remains partially undefined. Thus, although millimolar concentrations of FBP modulate *in vivo* and *in vitro* CggR's DNA binding activity, also here a direct proof of FBP-binding to CggR at this physiological concentrations of the metabolite is still missing.

Here, given the recently recognized importance of the flux-signaling metabolite FBP, we wanted to clarify if the glycolytic flux signal in the form of FBP is indeed transduced through the TFs Cra and CggR to generate a flux-dependent cellular response. Using thermal shift assays (TSA) and microscale thermophoresis (MST), we demonstrate that FBP does not bind Cra even at millimolar concentrations of the metabolite, and show that also in *E. coli* F1P is the only effector of Cra. In contrast, we show that FBP does bind CggR within the physiological concentration range of FBP (i.e., 0.5 to 10 mM). Electrophoretic mobility shift assays further confirmed an FBP concentration-dependent reduction in CggR affinity in the same concentration range, thus revealing that the interaction between the transcriptional repressor and FBP modulates its DNA-binding activity. Thus, in this work, we rule out a direct regulation of the transcription factor Cra by the flux-signaling metabolite FBP in *E. coli*, but show that glycolytic flux information is transduced through binding of FBP to CggR in *B. subtilis*. Untangling how metabolic fluxes are sensed and transduced is crucial to understand essential aspects of cell physiology (Papagiannakis *et al.*, 2017) and for metabolic engineering (Lehning *et al.*, 2017).

Results

FBP neither binds nor regulates the E. coli *Cra*

It has been previously suggested that F1P traces contained in commercial FBP might explain the observed FBP regulation of Cra (Ramseier *et al.*, 1993; Chavarría

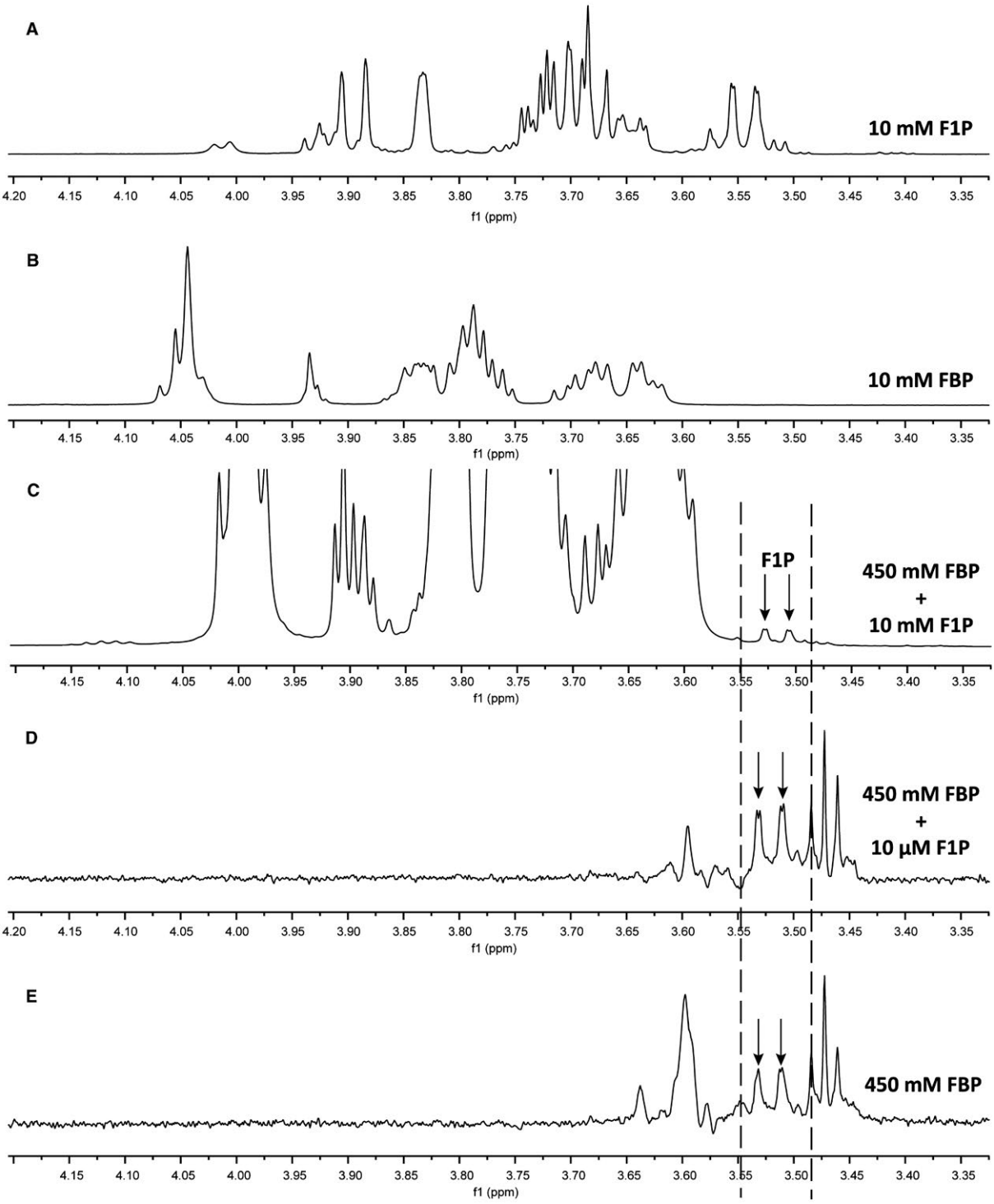

Fig. 1. The FBP samples tested contained less than 0.002% of F1P.
A. ^{1}H-NMR spectrum of F1P (10 mM).
B. ^{1}H-NMR spectrum of FBP (10 mM).
C. ^{1}H-NMR spectrum of FBP (450 mM) with F1P (10 mM).
D. ^{1}H-NMR spectrum of FBP (450 mM) with F1P (10 µM).
E. ^{1}H-NMR spectrum of FBP (450 mM) only. The black arrows indicate the F1P peaks present in the selected region.

et al., 2011). To avoid any confounding influence of F1P in our study, we used selective excitation NMR (Stott *et al*., 1995) to quantify F1P traces in our FBP solution. In specific, we first determined F1P and FBP proton spectra separately, and then selected a region with clear peaks in the F1P spectrum and no peaks from the FBP spectrum for our further analyses (Figure 1A-C). Using this region, we could only detect very weak F1P signals in a concentrated 450 mM FBP solution, which we estimated to correspond to a concentration of F1P of 9 µM (Figure 1D-E). Thus, our FBP solution contained an F1P contamination of less than 0.002%.

To investigate whether there is binding between Cra and FBP at physiological FBP levels and in cytoplasmic-like conditions, we used thermal shift assays (TSA), as this method tolerates complex buffers and high ligand concentrations (Grøftehauge *et al*., 2015). Ligand-binding may alter the thermal denaturation of a protein, which can be assessed in TSA by determining the change in protein's melting temperature (T_m) in the presence of the ligand. Indeed, with the *bona fide* ligand of Cra, F1P, we found that increasing concentrations of F1P induced a gradual increase of Cra's T_m up to 10°C (Figure 2A). In control experiments, we verified that the observed effects were not due to changes in ionic strength induced by the simultaneous titration of the F1P counter ions (2 K^+ per F1P molecule) (Figure 2A and B, Supplementary Figure 1). With FBP, we observed a 1.5°C decrease in the T_m of Cra only at the highest concentration point of the titration (30 mM) that cannot be attributed to the total increase in the Na^+ counter ion concentration (Figure 2B). However, the amplitude of this change is very small (1.5°C compared to 10°C with F1P), and we observed an increase in a similar magnitude in the presence of mannose-6-phosphate (Supplementary Figure 1), used here as a negative control, suggesting that these changes would mainly reflect unspecific binding events. Therefore, TSA provided no evidence that supports FBP binding to Cra.

Since we cannot rule out that FBP-binding induces only slight conformational changes not detectable by TSA, we further tested for binding between FBP and Cra using microscale thermophoresis (MST). Thermophoresis, the directed motion of a molecule in a temperature gradient, is highly sensitive to all kinds of binding-induced changes of molecular properties, such as size, charge or hydration shell, which can be monitored by different parameters (fluorescence, thermophoresis, temperature jump) (Jerabek-Willemsen *et al*., 2011). Using this technique, we found that the fluorescence of Alexa-647-labeled Cra was quenched in the presence of F1P in a concentration-dependent manner (Figure 2C). Because fluorescence stays constant when using denatured Cra in these binding

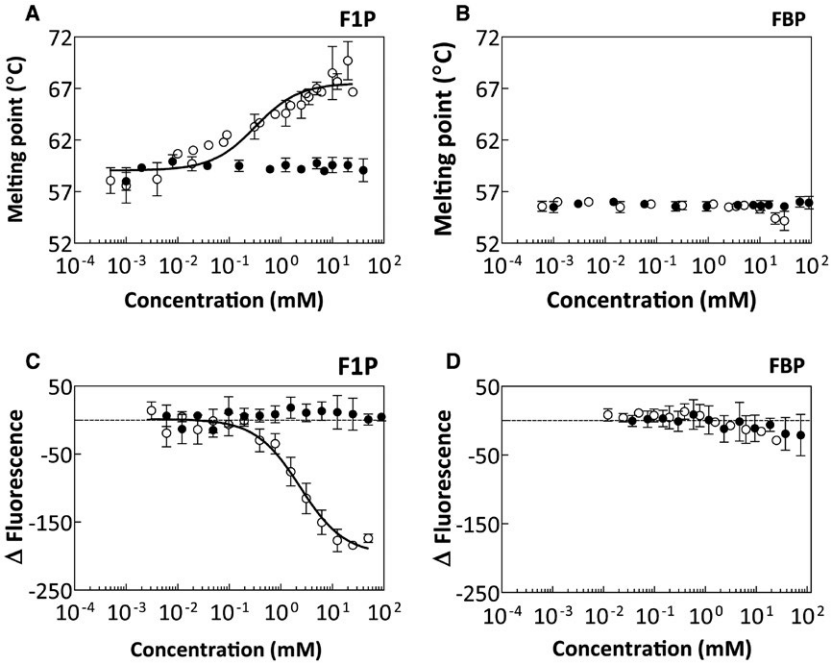

Fig. 2. FBP does not bind *E. coli* Cra. Thermal shift assays (TSA) of Cra in presence of F1P (**A**) and FBP (**B**) (open circles). Titrations of K^+ (KH_2PO_4) and Na^+ (NaH_2PO_4) counter ions present F1P and FBP salt solutions respectively (closed circles). Points represent the mean and standard deviation of six (for F1P) and ten replicates (for FBP). Binding experiments of Cra and F1P (**C**), and Cra and FBP (**D**) as determined by microscale thermophoresis (MST). Plotted is the fluorescence of Cra labeled with Alexa-647 in presence of different concentrations of the metabolites F1P and FBP (open circles) or their respective counter ions (closed circles). MST measurements were performed in triplicate and the errors are given in standard deviation. The x-axes in all plots represent the concentrations of the metabolites or the respective KH_2PO_4 or NaH_2PO_4 control solutions.

experiments (Supplementary Figure 2), the observed quenching must correspond to structural changes of native Cra resulting from F1P-binding. Also, the increase in K^+ counter ions titrated along with F1P did not affect the fluorescence signals of labeled Cra (Figure 2C).

In contrast, we found no significant changes in the fluorescence of Cra in the presence of FBP (Figure 2D). Other parameters as quantified with MST showed only slight alterations at the highest concentrations of FBP tested (from 3 to 25 mM) (Supplementary Figure 3A-B). This observation is consistent with the results obtained with TSA and, together with the strong effect seen with F1P, support the notion that these changes only arise from non-specific interactions occurring at very high concentration of the FBP. Therefore, although it has been previously reported that addition of millimolar concentrations of FBP reverses binding of Cra to its operator sites (Ramseier *et al.*, 1993; Ramseier *et al.*, 1995), neither our TSA nor MST support a direct interaction between FBP and Cra.

To resolve this discrepancy with the previous reports, we investigated the effect of FBP on Cra-binding to its DNA operator by electrophoretic mobility shift assays (EMSA). Here, we incubated a labeled DNA fragment containing Cra's operator with Cra in the presence of different concentrations of FBP, F1P (positive control) or mannose-6-phosphate (M6P) (negative control), and resolved DNA-protein complexes and free DNA by electrophoresis in native conditions (Figure 3A, Supplementary Figure 4). Here, the addition of F1P gradually shifted the band in a concentration-dependent manner (Figure 3A – lanes 9 to 12). In contrast, FBP induced a faint increase in the intensity of lower band only at the highest concentrations of FBP tested (Figure 3A, Supplementary Figure 4). We did not observe a similar decrease in the presence of the same concentrations of M6P (Supplementary Figure 4), which suggests that indeed F1P traces in our FBP solution (0.4 µM F1P in 20 mM FBP) could underlie this partial release of Cra from its operator. Together, these results demonstrate that FBP does not bind Cra nor allosterically regulates the affinity for its operator DNA sequence.

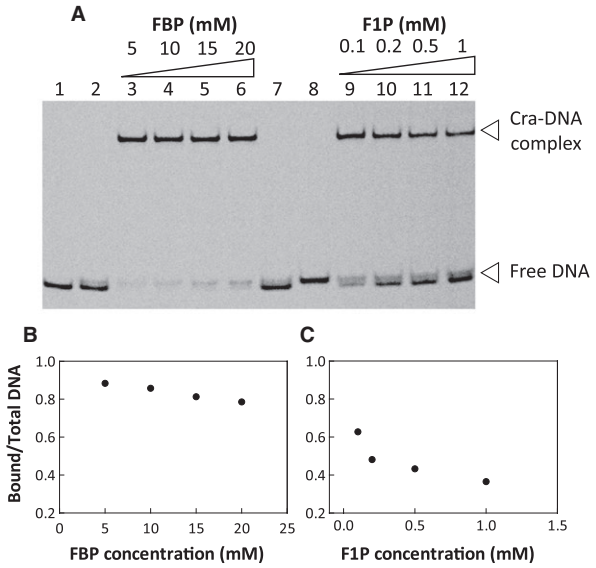

Fig. 3. F1P is responsible for regulating the interaction of Cra and the DNA operator, while FBP only shows a slight effect, most likely due to an unspecific effect.
A. EMSA analyzed with 5% TBE polyacrylamide gel electrophoresis. Lane 1: Cra DNA operator sequence. Lane 2: Cra DNA operator sequence + BSA. Lanes 3 – 6: Cra DNA operator sequence + Cra + different concentrations of FBP. Lane 7: Random DNA sequence. Lane 8: Random DNA sequence + Cra. Lanes 9 – 12: Cra DNA operator sequence + Cra + different concentrations of F1P.
B. and C. Quantification analysis of the DNA bands from the experiments with FBP and F1P. In these analysis, using ImageJ, each lane of the gel was selected and the area of each band estimated. The value of the upper bands, representing the DNA/Cra complexes, were divided by the sum of the upper (bound DNA) and both lower bands (free DNA).

FBP binds and regulates CggR at millimolar concentrations

To determine whether FBP binds to CggR in the physiological millimolar concentration range of the metabolite, we also first used TSA. In this case, FBP triggered a concentration-dependent increase in CggR's T_m up to 6.9°C not related to the co-titration of Na^+ counter ion (three molecules of Na^+ per molecule of FBP), indicating occurrence of structural changes associated to FBP-binding (Figure 4A). Remarkably, these changes occurred over a concentration range (from 100 µM to 30 mM, Figure 4A) where the known high affinity binding site ($K_D \approx 6$ µM, (Zorrilla, Chaix, *et al.*, 2007)) would long be saturated.

We next used MST to further confirm this binding of FBP with CggR at millimolar FBP concentrations. Here, we found that both CggR's temperature jump (T-jump) and thermophoretic mobility were altered in the presence of FBP (Figure 4B, Supplementary Figure 5). Control experiments with sodium phosphate also showed a concentration-dependent decrease in the T-jump but considerably smaller than that caused by FBP (Figure 4B, Supplementary Figure 5), which supports that FBP binds CggR within mM concentration range. Characterization of the affinity using a simple model based on the mass-action law retrieved comparable values for the apparent K_D from both the TSA and MST data (2.54 and 1.19 mM respectively; Table 1). Thus, these experiments revealed a direct interaction of FBP with CggR in the millimolar concentration range of the metabolite.

To determine the functional role of the observed interaction of FBP with CggR, we examined the effect millimolar FBP concentrations on DNA-binding activity of CggR

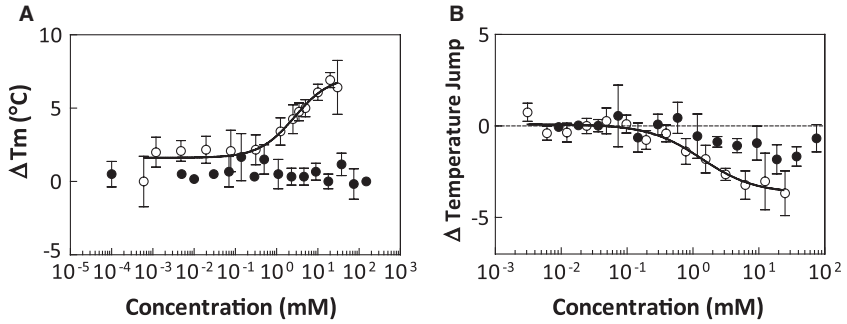

Fig. 4. FBP binds CggR within millimolar concentration range of the metabolite.
A. The melting point (T_m) of CggR was determined in presence of FBP (open circles) or NaCl solutions (closed circles) used as control for the presence of the three sodium counter ions in FBP salts. Points represent the mean of six (FBP) and three (NaCl) experiments, and the error bars the standard deviation.
B. Microscale thermophoresis (MST) analysis of temperature jump of CggR in presence of different concentrations of FBP (open circles) and of NaH_2PO_4 solutions, as control (closed circles). Points represent the mean of four (FBP) and three (NaH_2PO_4) experiments, and the errors the standard deviation. The x-axis in both graphs describes the concentrations of FBP and the concentrations of the NaH_2PO_4 control solutions.

using EMSA. In particular, a DNA fragment labeled with Alexa-647 containing the operator sequence from the gapA operon (Doan and Aymerich, 2003) was incubated with CggR in the presence of physiological concentrations of FBP (5–20 mM). Here, we observed that FBP progressively reversed CggR's shifted band in a concentration-dependent manner down to 60% at 20 mM FBP (Figure 5A-B). In contrast, the band corresponding to the DNA-CggR complex remained unchanged in the presence of the same concentrations of the phosphorylated sugar M6P (Figure 5A). As the Na^+ counter ion in the FBP salt solution is co-titrated along with FBP, causing its concentration to rise up to 70 mM (10 mM from the buffer + 60 mM from 20 mM FBP concentration point), we next checked whether this increase could partially shield ionic interactions between CggR and its operator site and thus de-stabilize the DNA-protein complex irrespective of FBP. Here, when we titrated only the Na^+, we did not observe changes in the shifted band (Supplementary Figure 6). Further, FBP-induced band shift reversion was also evident when we corrected for the salt content to precisely have the same concentration of Na^+ (i.e., 100 mM) in every point in the FBP titrations (Supplementary Figure 6), which indicates that the differences in Na^+ concentration did not play any role in the dissociation of CggR-DNA complex. Thus, collectively, these results show that FBP binds CggR at millimolar concentration, and that this interaction allosterically regulates DNA-binding activity of this transcription factor at physiological FBP concentrations.

Table 1. Estimation of apparent binding affinity (K_D) of CggR and FBP. IQR, interquartile range on measurement errors as determined by bootstrapping. S.E, standard error of the fit.

Method	K_D ± IQR (mM)	S.E.
Thermal shift assay	2.54 ± 0.17	0.02
MST – thermophoresis	1.24 ± 0.36	0.04
MST – temperature jump	1.19 ± 0.47	0.03

Previous work has described that, *in vitro*, micromolar concentrations of FBP prevent high order oligomerization of CggR (Zorrilla, Chaix, *et al*., 2007), while millimolar concentrations are necessary to impair binding to the operator sequence (Doan and Aymerich, 2003; Zorrilla, Doan, *et al*., 2007). To explain these FBP concentration-dependent effects of FBP *in vitro*, it has been proposed that two sugar binding sites exist in CggR, from which only one has been identified thus far (Zorrilla, Doan, *et al*., 2007; Zorrilla, Chaix, *et al*., 2007; Doan *et al*., 2008; Řezáčová *et al*., 2008). Towards identifying the potential second FBP binding site, we performed a molecular docking study. In the published structure (3BXF) (Řezáčová *et al*., 2008), CggR is a homodimer, in which FBP binds in subunit A, while dihydroxyacetonephosphate binds in subunit B at the same site (Supplementary Figure 7A). We started by removal of the two ligands from the structure and then performed 800 docking runs with FBP as the ligand. Here, we found that FBP binding occurred 720 times in the already known binding site of subunit A and 80 times in the corresponding site in subunit B (Supplementary Figure 7B). We found that the predicted FBP binding positions in subunit A all had steric overlap with the experimentally observed position of the FBP in the X-ray structure. The docking never predicted that binding would occur outside the already known binding site. As an extra control, given that FBP is strongly negatively charged, we also inspected an electrostatic surface map of CggR to search for sites with a positive charge. The only sites in the dimer that were conspicuously positively charged were the known

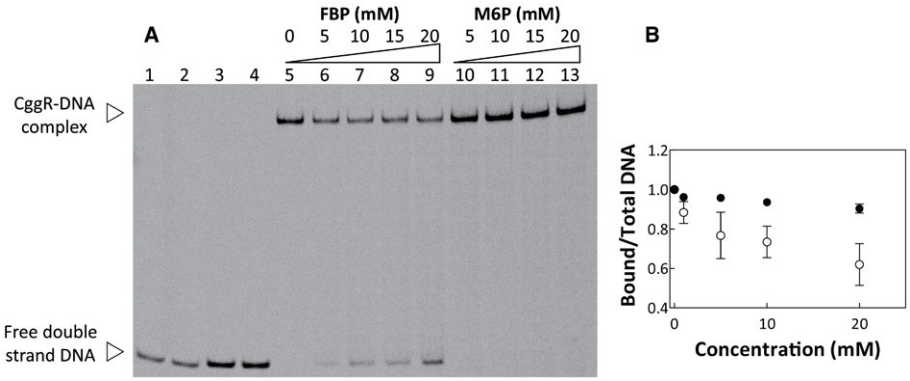

Fig. 5. FBP interaction with CggR at millimolar concentration impairs CggR's DNA-binding activity.
A. EMSA of CggR-DNA operator binding in the presence of FBP or M6P. Lane 1: Random DNA sequence. Lane 2: Random DNA sequence + CggR. Lane 3: CggR DNA operator sequence. Lane 4: CggR DNA operator sequence + BSA. Lane 5 – 9: CggR DNA operator sequence + CggR + different concentrations of FBP. Lanes 10 – 13: CggR DNA operator sequence + CggR + different concentrations of M6P.
B. Quantification analysis of the DNA bands from the experiments with FBP (open circles) and M6P (closed circles). Bound/Total DNA corresponds to the intensity of the upper band (DNA-CggR complexes) divided by the sum of the intensities of the upper (bound DNA) and lower bands (free DNA). Points represent the mean of three replicates of FBP experiments and two replicates for M6P experiments. Error bars correspond to the standard deviation.

binding sites. These results do not support the occurrence of a second binding site, and suggest that the binding site identified in the structure and docking studies is the only FBP-binding site in CggR.

Discussion

Here, using a set of biochemical techniques we investigated the binding of the flux-signaling metabolite FBP (Kochanowski *et al.*, 2013) to the global transcription factors Cra of *E. coli* and CggR of *B. subtilis*. While to the best of our knowledge the only published evidence for the FBP-Cra interaction is a band shift assay where 5 mM FBP induced a modest release of Cra from a 210 bp DNA fragment of *ppsA* promoter (Ramseier *et al.*, 1993), it is widely considered that FBP binds and allosterically regulates this transcription factor (Ramseier *et al.*, 1993; Ramseier *et al.*, 1995; Saier and Ramseier, 1996; Kotte *et al.*, 2010; Kochanowski *et al.*, 2013; Chubukov *et al.*, 2014; Lehning *et al.*, 2017). However, here, we could not find any evidence that demonstrates binding of FBP to *E. coli*'s Cra, while with the two different techniques used (TSA and MST) we confirmed F1P-binding to Cra, and FBP-binding to *B. subtilis* transcription factor CggR. In addition, band shift experiments indicated a consistent effect on DNA-binding activity of Cra by F1P and of CggR by FBP, while FBP failed to impair DNA-Cra complex formation. Thus, our analyses demonstrate that FBP neither binds nor regulates Cra DNA-binding activity *in vitro* and thus, is not a direct allosteric regulator of this transcription factor in *E. coli*.

Ramseier *et al.* suggested that it cannot be ruled out that F1P traces in FBP solutions might be responsible for the weak effect they observed when using millimolar concentrations of FBP (Ramseier *et al.*, 1993; Ramseier *et al.*, 1995). In agreement with this possibility, Chavarría *et al.* found only F1P associated with Cra after soaking the protein crystal in a 1 mM FBP solution (Chavarría *et al.*, 2011). However, no one has ever measured these traces, and thus this hypothesis could not be verified. Here, we quantified F1P traces in our FBP solution and found two molecules of F1P per 100,000 molecules of FBP. As the efficient concentration of F1P needed to dissociate DNA-Cra complex is in the micromolar range (Fig. 3, (Ramseier *et al.*, 1993)), F1P traces present in our FBP solution are largely insufficient to regulate Cra. Consistently, we observed an extremely small impairment of Cra's DNA-binding activity only at the highest concentrations of FBP (20–30 mM). As this impairment did not happen in presence of the same concentrations of another phosphorylated sugar (mannose-6-phosphate), this suggests that the minimal F1P traces (e.g., 0.6 μM F1P in 30 mM FBP) are responsible for this effect. Therefore, although F1P impurities in FBP solution used by Ramseier are not known, our results suggest that the changes of Cra's affinity for its operator observed by these authors must indeed had been due to the presence of higher amounts of contaminating F1P.

Other contaminants, also present in binding assays, could also have influenced previous experiments (Wei *et al.*, 2016; Zhu *et al.*, 2016). For instance, counter ions present in phosphorylated metabolite salt solutions introduced along with the ligand might affect electrostatic interactions involved in ligand–protein or protein–DNA contacts. In addition, ligands with ionizable groups at high concentration might exceed the buffering capacity, and

consequently change the pH of the buffer. pH adjustment of ligand stock solution in turn will change final ions concentration (for instance, Na^+ when using NaOH). Here, we adjusted the pH, recalculated the resulting ion concentration in our metabolite solutions, and performed control experiments, in which we exclusively assessed the effect of the different salt concentrations on binding. Therefore, it is possible that observed effects in ITC experiments (cf. Wei *et al.*, 2016; Zhu *et al.*, 2016), or on Cra DNA-binding activity (cf. (Ramseier *et al.*, 1993; Ramseier *et al.*, 1995)) could also have resulted from effects of contaminant molecules (e.g., F1P, Na^+, H^+), titrated along with FBP.

In our prior work, we had found that *in vivo* the activity of Cra inversely correlates with intracellular FBP concentration and glycolytic flux, independently on the carbon source or cultivation condition used (Kochanowski *et al.*, 2013), and we had proposed that FBP is a signal for glycolytic flux that would regulate Cra activity in a flux-dependent manner. But if FBP is now not the regulator of Cra, why did we still observe glycolytic flux-dependent Cra activity (Kochanowski *et al.*, 2013)? F1P is believed to be solely generated upon fructose uptake through the FruBA phosphotransferase system (Kornberg, 2001). Thus, how could the observed glycolytic-flux dependence Cra regulation take place *in vivo*? A recent systems-level analysis found that cyclic AMP, FBP and F1P alone explained most of the specific transcriptional regulation in *E. coli* through their interaction with the two major transcription factors Crp and Cra (Kochanowski *et al.*, 2017). Strikingly, among 47 central metabolites F1P displayed the highest intracellular concentration variance across 23 different growth conditions and a highly significant direct correlation with FBP (Kochanowski *et al.*, 2017), indicating that F1P is produced in *E. coli* also in conditions other than growth in fructose as the only carbon source. In this regard, a recent work described that the enzyme FruK can work reversibly and convert FBP into F1P (Singh *et al.*, 2017). Interestingly enough, the same work reports that FruK interacts with Cra *in vivo*, and that conversion FBP into F1P regulates Cra/FruK affinity for Cra's DNA operators *in vitro* (Singh *et al.*, 2017). Thus, these results raise an interesting scenario where, similarly to cAMP or fructose-2,6-bisphosphate (in mammals), F1P would act as a second messenger (that is, not involved directly in central metabolism) to relay metabolic fluxes into a physiological response, via regulation of Cra.

Next to Cra, in this work, we also performed a biochemical characterization of the interaction between FBP and CggR. Previous studies have shown that *in vitro* FBP acts as a structural cofactor at micromolar FBP concentration and as a inducer at millimolar (Zorrilla, Doan, *et al.*, 2007; Zorrilla, Chaix, *et al.*, 2007). In order to explain this potential dual effect of the interaction of FBP with CggR, it has been argued that CggR possesses two distinct sugar-binding sites with different affinities (Zorrilla, Chaix, *et al.*, 2007). In this work, we demonstrate that FBP binds CggR at millimolar concentration and also releases the transcription factor from its DNA operator at this concentration, but we could not find a second FBP-binding site different to the one experimentally identified and earlier characterized as the 'high affinity site' (Řezáčová *et al.*, 2008). Moreover, we found no positively charged surface areas other than the known FBP-binding site that might accommodate a phosphorylated metabolite. Consistently, Řezáčová *et al.* found a unique binding site in CggR crystals even when co-crystallizing the native protein in the presence of 90 mM FBP (Řezáčová *et al.*, 2008). In this site, FBP establishes ionic interactions with Arg175 (Řezáčová *et al.*, 2008). CggR point mutant seems to have lost the cooperative binding to the operator DNA, is not sensitive by FBP regulation, and behaves as inactive repressor *in vivo* (i.e., constitutive expression of reporter gene under both glycolytic and gluconeogenic growth conditions) (Doan *et al.*, 2008), indicating that FBP interaction at the known binding site underlies its activity as inducer. Thus, there is no experimental evidence that supports the existence of a second FBP-binding site in CggR and we conclude that the earlier reported 'high affinity' site is the only FBP-binding site in CggR, to which we find FBP to bind in the millimolar range.

Although previous work has demonstrated that FBP can bind CggR *in vitro* at concentrations much lower than the physiological one, the role of this interaction *in vivo* is not clear. In this regard, monophosphorylated metabolites (eg, dihydroxyacetone phosphate, glucose-6-phosphate and fructose-6-phosphate) can bind CggR with high affinity to the same site as FBP, also without altering CggR's DNA-binding activity (Doan *et al.*, 2008; Řezáčová *et al.*, 2008). This poor selectivity, the fact that the physiological concentration of these metabolites is much higher the affinity determined by ITC (Zorrilla, Chaix, *et al.*, 2007; Řezáčová *et al.*, 2008), and the lack of a functional consequence in CggR DNA-binding activity (Doan *et al.*, 2008) suggest that interactions at micromolar concentrations of the metabolites could only play an ancillary role *in vivo*.

In bacteria, intracellular concentration of most relevant metabolites typically ranges from hundreds of micromolar to millimolar (Bennett *et al.*, 2009; Meyer *et al.*, 2014). However, widely used benchmark methods for characterizing molecular interactions (e.g., isothermal titration calorimetry) are very sensitive to buffer mismatch (i.e., presence of additional ions or contaminant traces in the ligand solution) and are more suitable to quantitatively determine affinities from sub-nanomolar to the micromolar range, and thus are not optimal to assess allosteric interactions in the physiological concentrations ranges

Table 2. Composition of buffer used in this study.

Buffer	Composition	pH
Buffer A	Tris-HCl (50 mM) pH 7.2.	7
Buffer B	Tris-HCl (50 mM) pH 7.2, NaCl (150 mM).	7
Lysis buffer	Tris-HCl (50 mM) pH 7.2, NaCl (150 mM), EDTA (1 mM), PMSF (1 mM), $MgCl_2$ (15 mM) and DNAse (10 μg mL^{-1}).	7
Cytosolic buffer	KH_2PO_4 (6 mM), K_2HPO_4 (14 mM); KCl (140 mM), glucose (5.5% w/v), $MgCl_2$ (5 mM), NaCl (10 mM). The pH was adjusted with 1M KOH.	7
Modified cytosolic buffer	KH_2PO_4 (6 mM), K_2HPO_4 (14 mM), KCl (140 mM), NaCl (250 mM). The pH was adjusted with a 1M KOH solution.	7
EMSA binding buffer	NaH_2PO_4 (10mM), NaCl (100mM), EDTA (1mM), DTT (1mM), glycerol (5%). The pH was adjusted with 1M KOH .	7.8

of metabolites of primary metabolism. Here, using two biophysical techniques (MST and TSA) that are more appropriate to deal with complex buffers and high ligand concentrations (and an adequate set of controls) we clarified conflicting results and unanswered questions relevant for the regulation of two global bacterial transcription factors of carbon metabolism. In summary, this work contributes to understand fundamental questions about the regulation of Cra and CggR, clarifying long standing questions about binding partners and binding affinities.

Experimental procedures

Chemicals

D-Fructose-1,6-bisphosphate trisodium salt (FBP) 99% pure (MF03222) and D-mannose-6-phosphate disodium salt hydrate (M6P) 95% pure (MM05046) were purchased from Carbosynth (UK); D-Fructose 1-phosphate dipotassium salt (F1P) 99% pure from Santa Cruz (Dallas, TX) (sc-500907A); and salmon sperm DNA from Sigma-Aldrich (D1626-1G).

The composition of all the buffers used are described in the Table 2.

Selective excitation NMR

Solutions of FBP and F1P were prepared in D_2O and the spectra of FBP (10 mM) and F1P (10 mM) determined separately. The region selected for selective excitation displaying signals for F1P but not for FBP was centered at 3.51 ppm with a width of 60.1 Hz. The detection limit of this method was estimated with samples prepared by mixing a high concentration of FBP (450 mM) with low concentration of F1P (10 μM), and F1P traces were assessed in a 450 mM FBP solution. During the selective excitation, ^{13}C decoupling was used to suppress the ^{13}C satellites of FBP. A relaxation time of 2 sec and an acquisition time of 1 sec were used. NMR spectra were zero filled once, and multiplied by an exponential line broadening function of 0.5 Hz prior to Fourier transformation. The number of scans used for the samples containing 450 mM FBP, and 450 mM of FBP in combination with 10 μM of F1P, was 1,024. For the samples containing 10 mM FBP and the sample with 10 mM F1P, 8 scans were used. The spectra were manually processed in MestReNova.

Protein expression and purification

Cra from *E. coli* was cloned in vector pBAD with a *C*-terminal His_{10}-tag, and expressed in the *E. coli* strain MC1061, using an earlier described methodology (Geertsma and Poolman, 2007). The primers used are described in the Supplementary Table 1. The synthetic gene CggR was purchased from Life Technologies (Carlsbad, CA), and cloned in pET100/D-TOPO (Thermo Fisher Scientific; Waltham, MA), with an N-terminal His_6-tag. All constructs were verified by Sanger sequencing. For protein production, a single colony was used to inoculate 50 mL LB containing 100 μg mL^{-1} ampicillin, and the culture grown at 37°C overnight. This culture was diluted to an optical density (OD_{600}) of 0.05 in a final volume of 1 liter. Protein expression was induced at OD_{600} 0.5 by addition of L-arabinose (0.01% v/v) (for Cra) or 10 μM IPTG (for CggR), and the cells subsequently grown at 30°C and 180 rpm for four more hours. Cells were harvested by centrifugation at 6,600xg at 4°C for 20 min, washed once in modified cytosolic buffer (Table 2), and the pellet was frozen in liquid nitrogen and stored at -80°C.

For protein purification, cell pellets were resuspended in chilled lysis buffer (Table 2) and lysed by high-pressure disruption (Constant Cell Disruption System, Ltd, UK) in one passage at 25 Kpsi at 4°C. Lysate was cleared by centrifugation at 30,000xg (Beckman JA-17 rotor), and incubated in batch with 0.5 mL of nickel-sepharose resin (pre-equilibrated with buffer A (Table 2)) at 4°C for 1 h. Subsequently, the suspension was poured onto a 10 mL disposable column (Bio-Rad), and the settled resin washed with 20 column volumes of buffer B containing imidazole (50 mM), followed by 20 column volumes of buffer B containing L-histidine (50 mM).

Proteins were eluted using modified cytosolic buffer supplemented with 235 mM L-histidine. The fractions containing the target protein were loaded on a Superdex 200 10/300 gel filtration column (GE Healthcare), using cytosolic buffer as column buffer. After gel filtration the fractions containing the proteins were stored at 4°C until use.

Thermal shift assays (TSA)

Samples of 25 µL (final volume) were prepared in ice, and contained 5 µL of 5x SYPRO Orange (Molecular Probes; Eugene, OR), 1 µL of 1 mg mL^{-1} of the purified protein diluted in cytosolic buffer, and different concentrations of the metabolites (FBP, F1P or M6P) in cytosolic buffer. In control experiments aimed to test the effect of counter ions present in metabolites' salt solutions, NaCl (for FBP and M6P) and KH_2PO_4 (for F1P) solutions prepared with cytosolic buffer were added instead of the corresponding metabolite to a final concentrations twice (for F1P and M6P) or three times (for FBP) as big as the concentration of the metabolite in each corresponding point. Samples were transferred into 96 thin-well PCR plates (Bio-Rad), the plates sealed with Optical-Quality Sealing Tape (Bio-Rad), and then analyzed in a CFX96 Real-Time System combined with C1000 Touch Thermal Cycler (Bio-Rad). Analysis consisted of a single heating cycle from 20°C to 95°C with increments of 0.5°C steps followed by fluorescence intensity monitoring with a charge-coupled device camera. The wavelengths for excitation and emission were 490 and 575 nm respectively. The T_m was automatically calculated by the control software and corresponded to the local maximum of the first derivative of measured fluorescence versus temperature.

Microscale thermophoresis (MST)

Purified CggR and Cra were labeled with Alexa-647 using the protein labeling NHS RED Kit (NanoTemper Technologies, Munich, Germany) as described by the manufacturer. The final concentrations of total (12.8 and 6.6 µM) and labeled (8 µM and 4 µM) CggR and Cra in modified cytosolic buffer (Table 2) were determined from the absorbance at 280 and 647 nm respectively, using a NanoDrop (Thermo Fisher Scientific; Waltham, MA). Protein parameters (extinction coefficient at 280 nm and molecular weight) were calculated with ProteinParam tool (https://web.expasy.org/protparam/) using protein sequences retrieved from Uniprot (Cra, P0ACP1; CggR, O32253).

Prior to MST measurements, labeled proteins were diluted 1:40 in cytosolic buffer containing Tween 20 (0.05% w/v). Samples were prepared by mixing a volume of 5 µL of the diluted labeled protein with 5 µL of a series of FBP dilutions (two-fold serial dilution starting at 50 mM), for CggR, and F1P or FBP, for Cra, prepared in modified cytosolic buffer. The final concentrations of labeled Cra and CggR in the assay were 100 and 50 nM respectively. For MST measurements, samples were loaded in "premium coated capillaries" and analyzed in a MST Monolith NT.115 (both from NanoTemper Technologies; Munich, Germany) at 25°C, using 60% LED power and 40% IR-laser power. In control experiments with denatured Cra, before sample preparation the protein was denatured with 7 M of urea and 1 mM DTT, and boiled for 10 minutes. In control experiments to assess the influence of counter ions in metabolite salt solutions the labeled proteins were added to a series of dilutions of KH_2PO_4 or NaH_2PO_4 solutions prepared in cytosolic buffer (corresponding to K^+ present in F1P and Na^+ present in FBP and M6P solutions respectively). The concentration range of each salt solution tested in these experiments was adjusted to the number of counter ions molecules co-titrated with the corresponding metabolite in binding experiments (i.e., three molecules of Na^+ per molecule of FBP, and two molecules K^+ and Na^+ per molecule of F1P and M6P respectively).

Results from MST parameters (fluorescence, thermophoresis, and temperature jump) measurements were exported using the NTA Analysis software (NanoTemper Technologies) and normalized (Δ-fluorescence, Δ-thermophoresis, Δ-temperature jump) by substracting the average of the three values of the lowest F1P, FBP, KH_2PO_4 or NaH_2PO_4 concentrations (including 0 mM, where only the buffer was added) from all measured values.

Binding data analysis

To estimate the parameters of FBP-CggR binding reactions we used the quadratic resolution of the law of mass action (Eq. 1). We used this equation because the final concentration of the labeled protein (0.16 µM for MST and 1.0 µM for TSA) is close to the previously reported K_D for FBP of the high affinity site (Zorrilla, Chaix, *et al.*, 2007; Řezáčová *et al.*, 2008).

Equation 1:

$$\text{Fraction bound} = \frac{1}{2C_A^0}\left(C_T^0 + C_A^0 + K_D - \sqrt{\left(C_T^0 + C_A^0 + K_D\right)^2 - 4C_T^0 C_A^0}\right)$$

Here, C_A^0 refers to the concentration of fluorescently labeled CggR; C_T^0 refers to the concentration of titrated molecule FBP and K_D is the dissociation constant, which is the parameter we want to estimate. To calculate the *fraction bound* we normalized T_m and Δ-thermophoresis and Δ-temperature jump values with regard to unbound and bound stages. Bound and unbound stages were calculated by averaging the results of two highest and three lowest dilutions of the ligand respectively. Each ligand dilution

point of the titration was normalized by subtracting from each value the one calculated for the unbound stage, and then this difference was divided by the difference between bound and unbound. The K_D values were fitted in Matlab using maximum likelihood estimation with measurement variance determined at each metabolite concentration. The interquartile range of the fitted K_D was obtained by bootstrapping on the measurement errors. The standard error of the fit is the standard deviation of the distances between the fitted curve and the mean of the data points at each ligand concentration.

Electrophoretic mobility shift assays (EMSA)

Fluorescently labeled DNA fragments used in EMSA were generated by hybridization of single-stranded forward (labeled with Alexa-Fluor-647 at the 5' end) and reverse (unlabeled) oligonucleotides containing the sequence of Cra or CggR operator sites or a random DNA sequence (Supplementary Table 2). CggR operator sequence corresponds to a synthetic CggR-responsive element that includes the four conserved nucleotide stretches (Zorrilla, Doan, *et al.*, 2007) separated by a randomized sequence of the same length as the non-conserved ones (Supplementary Note). Oligonucleotides were purchased from Integrated DNA Technologies (Coralville, IA), dissolved in 100 mM potassium acetate pH 7.5, 30 mM HEPES to a final concentration of 100 µM, mixed 1:1, and then incubated for 5 min at 95°C and cooled down at 1°C min^{-1} to room temperature. Hybridization efficiency was assessed by electrophoresis in native conditions. In specific, samples of the labeled single stranded oligonucleotide and from hybridized DNA were analyzed in 10% polyacrylamide gel in TBE, run with 0.5X TBE at constant voltage (14 V cm^{-1}) at room temperature. After migration, the gel was scanned in a Typhoon 9400, using the wavelengths 649 and 665 nm for excitation and emission respectively.

Hybridized labeled DNA fragments (final concentration 40 nM) were incubated 20 min at room temperature with 1 µM CggR, 0.5 µM Cra or 4 µM BSA, in the presence of different concentrations of the metabolites F1P (0.1, 0.2, 0.5 and 1 mM), FBP (5, 10, 15 and 20 mM) or M6P (5, 10, 15 and 20 mM) in a final volume of 25 µL in binding buffer (Table 2) including 1 µg of salmon sperm DNA. Free DNA was resolved from DNA-protein complexes by native electrophoresis at 4°C. In control experiments aimed to assess solely the influence of Na^+ counter ions co-titrated along with FBP we added NaCl instead of FBP to a final concentration of 3, 15, 30 and 60 mM. In control experiments where the concentration of Na^+ was equalized across all FBP concentration points, different amounts of NaCl were added to the binding reactions to complement Na^+ co-titrated along with FBP such that every reaction contained a total Na^+ concentration of 60 mM.

The background-subtracted total intensities of the protein-DNA complex and the free-DNA bands were determined, and bound DNA/total DNA was calculated by dividing the intensity of the protein-DNA complex band by the total DNA (i.e., the sum of the signal from the protein-DNA complex band plus the one from free-DNA). In cases where there are two bands corresponding to free DNA we considered both bands for the calculations.

Molecular docking and electrostatic surface potential calculation

Docking was performed using the 3BXF structure of CggR (Řezáčová *et al.*, 2008). To prepare the structure for docking, all water molecules, salt ions and existing ligands were removed. Point charges for the docked FBP ligand were assigned using AM1- BCC (Jakalian *et al.*, 2002). For the docking itself, the standard settings of AutodockVina were used (Trott and Olson, 2010). The volume of space that the ligand could visit during docking was defined as a rectangular box that extended at least 10 Å from each side of the protein. As a result, the FBP molecule could explore the entire CggR structure during docking. For a visual search for potential FBP binding sites, electrostatic surface potentials were calculated by YASARA using a Poisson-Boltzmann solvation model (Baker *et al.*, 2001; Krieger and Vriend, 2014).

Acknowledgements

This work has been supported by the European Union Seventh Framework Programme (FP7-KBBE-2013-7-single-stage) under grant agreement no. 613745 (PROMYS). B.B.F. was a recipient of the Brazilian Fellowship Science without Borders program, from the Brazilian National Council for Scientific and Technological Development (CNPq), process 245630/2012-0. We are grateful to Dr. Pierre Soule for providing help in the interpretation of MST results and analysis of binding experiments.

Author contributions

Conceived and designed the study: BBF, ADO, MH; Acquired the data: BBF, GH, SBV, HJW, PvdM; Analyzed and interpreted the data: BBF, ADO, GH, HJW, AMA, MH; Wrote the manuscript: BBF, ADO, MH.

References

Baker, N.A., Sept, D., Joseph, S., Holst, M.J., and McCammon, J. A. (2001) Electrostatics of nanosystems: application to microtubules and the ribosome. *Proc Natl Acad Sci USA* **98**: 10037–10041.

Bennett, B.D., Kimball, E.H., Gao, M., Osterhout, R., Dien, S. J. Van, and Rabinowitz, J. D. (2009) Absolute metabolite concentrations and implied enzyme active site occupancy in *Escherichia coli*. *Nat Chem Biol* **5**: 593–599.

Bledig, S.A., and Ramseier, T. M. (1996) Frur mediates catabolite activation of pyruvate kinase (pykF) gene expression in Escherichia FruR Mediates Catabolite Activation of Pyruvate Kinase (pykF) Gene Expression in *Escherichia coli*. *J Bacteriol* **178**: 280–283.

Cameron, A.D., Roper, D.I., Moreton, K.M., Muirhead, H., Holbrook, J.J., and Wigley, D. B. (1994) Allosteric activation in Bacillus stearothermophilus lactate dehydrogenase investigated by an X-ray crystallographic analysis of a mutant designed to prevent tetramerization of the enzyme. *J Mol Biol* **238**: 615–625.

Chaix, D., Ferguson, M.L., Atmanene, C., van Dorsselaer, A., Sanglier-Cianférani, S., Royer, C.A., and Declerck, N. (2010) Physical basis of the inducer-dependent cooperativity of the central glycolytic genes repressor/DNA complex. *Nucleic Acids Res* **38**: 5944–5957.

Chavarría, M., Durante-Rodríguez, G., Krell, T., Santiago, C., Brezovsky, J., Damborsky, J., and de Lorenzo, V. (2014) Fructose 1-phosphate is the one and only physiological effector of the Cra (FruR) regulator of Pseudomonas putida. *FEBS Open Bio* **4**: 377–386.

Chavarría, M., Santiago, C., Platero, R., Krell, T., Casasnovas, J.M., and Lorenzo, V. De (2011) Fructose 1-phosphate is the preferred effector of the metabolic regulator Cra of Pseudomonas putida. *J Biol Chem* **286**: 9351–9359.

Chubukov, V., Gerosa, L., Kochanowski, K., and Sauer, U. (2014) Coordination of microbial metabolism. *Nat Rev Microbiol* **12**: 327–340.

Chubukov, V., Uhr, M., Chat, L.L., Kleijn, R.J., Jules, M., Link, H., *et al.* (2013) Transcriptional regulation is insufficient to explain substrate-induced flux changes in *Bacillus subtilis*. *Mol Syst Biol* **9**: 709.

Doan, T., and Aymerich, S. (2003) Regulation of the central glycolytic genes in *Bacillus subtilis*: Binding of the repressor CggR to its single DNA target sequence is modulated by fructose-1,6-bisphosphate. *Mol Microbiol* **47**: 1709–1721.

Doan, T., Martin, L., Zorrilla, S., Chaix, D., Aymerich, S., Labesse, G., and Declerck, N. (2008) A phospho-sugar binding domain homologous to NagB enzymes regulates the activity of the central glycolytic genes repressor. *Proteins Struct Funct Genet* **71**: 2038–2050.

Dombrauckas, J.D., Santarsiero, B.D., and Mesecar, A. D. (2005) Structural basis for tumor pyruvate kinase M2 allosteric regulation and catalysis. *Biochemistry* **44**: 9417–9429.

Fung, E., Wong, W.W., Suen, J.K., Bulter, T., Lee, S., and Liao, J. C. (2005) A synthetic gene–metabolic oscillator. *Nature* **435**: 118–122.

Geertsma, E.R., and Poolman, B. (2007) High-throughput cloning and expression in recalcitrant bacteria. *Nat Methods* **4**: 705–707.

Grøftehauge, M.K., Hajizadeh, N.R., Swann, M.J., and Pohl, E. (2015) Protein-ligand interactions investigated by thermal shift assays (TSA) and dual polarization interferometry (DPI). *Acta Crystallogr Sect D Biol Crystallogr* **71**: 36–44.

Jakalian, A., Jack, D.B., and Bayly, C.I. (2002) Fast, efficient generation of high-quality atomic charges. AM1-BCC model: II. Parameterization and validation. *J Comput Chem* **23**: 1623–1641.

Jerabek-Willemsen, M., Wienken, C.J., Braun, D., Baaske, P., and Duhr, S. (2011) Molecular interaction studies using microscale thermophoresis. *Assay Drug Dev Technol* **9**: 342–353.

Kleijn, R.J., Buescher, J.M., Chat, L.L., Jules, M., Aymerich, S., and Sauer, U. (2009) Metabolic fluxes during strong carbon catabolite repression by malate in *Bacillus subtilis*. *J Biol Chem* **285**: 1587–1596.

Kochanowski, K., Gerosa, L., Brunner, S.F., Christodoulou, D., Nikolaev, Y.V., and Sauer, U. (2017) Few regulatory metabolites coordinate expression of central metabolic genes in *Escherichia coli*. *Mol Syst Biol* **13**: 903.

Kochanowski, K., Volkmer, B., Gerosa, L., Haverkorn van Rijsewijk, B.R., Schmidt, A., and Heinemann, M. (2013) Functioning of a metabolic flux sensor in *Escherichia coli*. *Proc Natl Acad Sci USA* **110**: 1130–1135.

Kornberg, H. L. (2001) Routes for fructose utilization by *Escherichia coli*. *J Mol Microbiol Biotechnol* **3**: 355–359.

Kotte, O., Zaugg, J.B., and Heinemann, M. (2010) Bacterial adaptation through distributed sensing of metabolic fluxes. *Mol Syst Biol* **6**: 355.

Krieger, E., and Vriend, G. (2014) YASARA View - molecular graphics for all devices - from smartphones to workstations. *Bioinformatics* **30**: 2981–2982.

Lehning, C.E., Siedler, S., Ellabaan, M.M.H., and Sommer, M. O. A. (2017) Assessing glycolytic flux alterations resulting from genetic perturbations in E. coli using a biosensor. *Metab Eng* **42**: 194–202.

Link, H., Fuhrer, T., Gerosa, L., Zamboni, N., and Sauer, U. (2015) Real-time metabolome profiling of the metabolic switch between starvation and growth. *Nat Methods* **12**: 1091–1097.

Litsios, A., Ortega, A.D., Wit, E.C., and Heinemann, M. (2017) Metabolic-flux dependent regulation of microbial physiology. *Curr Opin Microbiol* **42**: 71–78.

Ludwig, H., Homuth, G., Schmalisch, M., Dyka, F.M., Hecker, M., and Stülke, J. (2001) Transcription of glycolytic genes and operons in *Bacillus subtilis*: evidence for the presence of multiple levels of control of the gapA operon. *Mol Microbiol* **41**: 409–422.

Meyer, H., Weidmann, H., Mäder, U., Hecker, M., Völker, U., and Lalk, M. (2014) A time resolved metabolomics study: the influence of different carbon sources during growth and starvation of *Bacillus subtilis*. *Mol Biosyst* **10**: 1812–1823.

Murcott, T.H., Gutfreund, H., and Muirhead, H. (1992) The cooperative binding of fructose-1,6-bisphosphate to yeast pyruvate kinase. *EMBO J* **11**: 3811–3814.

Ormö, M., Bystrom, C.E., and Remington, S. J. (1998) Crystal structure of a complex of *Escherichia coli* glycerol kinase and an allosteric effector fructose 1,6-bisphosphate. *Biochemistry* **37**: 16565–16572.

Papagiannakis, A., Niebel, B., Wit, E.C., and Heinemann, M. (2017) Autonomous metabolic oscillations robustly gate the early and late cell cycle. *Mol Cell* **65**: 285–295.

Ramseier, T.M., Bledig, S., Michotey, V., Feghali, R., and Saier, M. H. (1995) The global regulatory protein FruR

modulates the direction of carbon flow in *Escherichia coli*. *Mol Microbiol* **16**: 1157–1169.

Ramseier, T.M., Nègre, D., Cortay, J.C., Scarabel, M., and Cozzone, a J., and Saier, M.H., (1993) In vitro binding of the pleiotropic transcriptional regulatory protein, FruR, to the fru, pps, ace, pts and icd operons of *Escherichia coli* and Salmonella typhimurium. *J Mol Biol* **234**: 28–44.

Řezáčová, P., Kožíšek, M., Moy, S.F., Sieglová, I., Joachimiak, A., MacHius, M., and Otwinowski, Z. (2008) Crystal structures of the effector-binding domain of repressor Central glycolytic gene Regulator from *Bacillus subtilis* reveal ligand-induced structural changes upon binding of several glycolytic intermediates. *Mol Microbiol* **69**: 895–910.

Saier, M.H., and Ramseier, T. M. (1996) The catabolite repressor/activator (Cra) protein of enteric bacteria. *J Bacteriol* **178**: 3411–3417.

Singh, D., Fairlamb, M.S., Harrison, K.S., Weeramange, C., Meinhardt, S., Tungtur, S., *et al.* (2017) *Protein-protein interactions with fructose-1-kinase alter function of the central Escherichia coli transcription regulator, Cra*. BioRxiv https://doi.org/10.1101/201277.

Stott, K., Stonehouse, J., Keeler, J., Hwang, T.-L., and Shaka, A. J. (1995) Excitation sculpting in high-resolution nuclear magnetic resonance spectroscopy: application to selective NOE experiments. *J Am Chem Soc* **117**: 4199–4200.

Trott, O., and Olson, A. J. (2010) AutoDock Vina: improving the speed and accuracy of docking with a new scoring function, efficient optimization, and multithreading. *J Comput Chem* **31**: 455–461.

Wei, L.N., Zhu, L.W., and Tang, Y. J. (2016) Succinate production positively correlates with the affinity of the global transcription factor Cra for its effector FBP in *Escherichia coli*. *Biotechnol Biofuels* **9**: 1–15.

Yu, P., and Pettigrew, D. W. (2003) Linkage between fructose 1,6-bisphosphate binding and the dimer-tetramer equilibrium of *Escherichia coli* glycerol kinase: critical behavior arising from change of ligand stoichiometry. *Biochemistry* **42**: 4243–4252.

Zhu, L.W., Xia, S.T., Wei, L.N., Li, H.M., Yuan, Z.P., and Tang, Y. J. (2016) Enhancing succinic acid biosynthesis in *Escherichia coli* by engineering its global transcription factor, catabolite repressor/activator (Cra). *Sci Rep* **6**: 1–11.

Zorrilla, S., Chaix, D., Ortega, A., Alfonso, C., Doan, T., and Margeat, E. (2007) Fructose-1, 6-bisphosphate Acts Both as an Inducer and as a Structural Cofactor of the Central Glycolytic Genes Repressor (CggR). *Biochemistry* **46**: 14996–15008.

Zorrilla, S., Doan, T., Alfonso, C., Margeat, E., Ortega, A., Royer, C.A., and Declerck, N. (2007) Inducer-Modulated Cooperative Binding of the Tetrameric CggR Repressor to Operator DNA. *Biophys J* **92**: 3215–3227.

Supporting information

Additional supporting information may be found online in the Supporting Information section at the end of the article.